EDGE PRESERVING GLOBAL CONSTRAST ENHANCEMENT FOR MULTISCALE TURBULENCE MITIGATION

M.Pavithra Devi[.1], T.Maragatham[2], Karthik.S[3]

ABSTRACT

The aim of image enhancement is to improve the interpretability or perception of information in images for human viewers, or to provide 'better' input for another automated image processing techniques. The Contrast Enhancement Turbulence Mitigation (CETM) techniques can manage the vagueness and ambiguity efficiently. Contrast enhancement is a powerful tool to represent and process human knowledge in form of image enhancement. The CETM algorithm enhances image contrast very effectively. Over the years, many researchers have provided insight into the physics of either the fog or turbulence but not both. Researchers have proposed methods to remove fog in images fast enough for real-time processing. In addition methods have been proposed by other researchers that address the atmospheric turbulence problem. In this paper, provide an analysis that incorporates both physics models: 1) fog and 2) turbulence. It is observed how contrast enhancements (fog removal) can affect image alignment and image averaging. In this paper, a new joint contrast enhancement and turbulence mitigation (CETM) method that utilizes estimations from the contrast enhancement algorithm to improve the turbulence removal algorithm. It provides a new turbulent mitigation object metric that measures temporal consistency.

INTRODUCTION

Distant objects present difficulties to photograph well. Seeing detail obviously requires lenses with a very long focal length, so small motions of the camera during exposure cause significant blur. But the most vexing problem is atmospheric haze which often leads to the majority of photons arriving from scattering in the intervening media rather than from the object itself. Quantization noise becomes a significant problem. Other noise characteristics of the sensor are also increased in the contrast expansion following haze removal. Variations air density also cause refraction thus photons cannot be counted on to most amateur photographs the mountain seems to simply disappear. Even with a long lens and tripod on a clear day, the haze precludes creating a clean image of the mountain.

To provide some understanding of the physical processes underlying optical extinction and optical turbulence-induced signal losses, with an eye towards providing the reader with the necessary tools to evaluate and predict anticipated laser communication system performance. Optical extinction is caused by absorption and scattering by molecules and aerosol particles, and we begin with a description of the basic physical principles behind these processes. There are different models in use for molecular extinction and for aerosol extinction, and we survey those that are the most useful in the prediction of signal loss. Next, atmospheric properties that lead to the formation of optical turbulence are discussed. A comprehensive set of optical turbulence models is provided to enable estimation of optical turbulence strength in all levels of the atmosphere. Behavior of the propagating signal beam in optical turbulence is discussed, which leads to expressions for estimating optical communication system bit error rates as a function of both communication system

Author for Correspondence:
[1]M.Pavithra Devi, PG Scholar/CSE, SNS College of Technology, Coimbatore, India, Email: Pavi.cs33@gamil.com
[2] T.Maragatham, AP/CSE, SNS College of Technology, Coimbatore, India, Email: tmaragatham@gmail.com
[3]Karthik.S, Prof &DEAN/CSE, SNS College of Technology, Coimbatore, India, Email: profkarthick@gmail.com

and optical turbulence parameters. Sufficient information is provided to allow both system designers and users to calculate anticipated system performance over a wide range of channel characteristics for ground-to-ground, ground-to-air/air-to-ground, and satellite uplink/downlink optical communication scenarios.
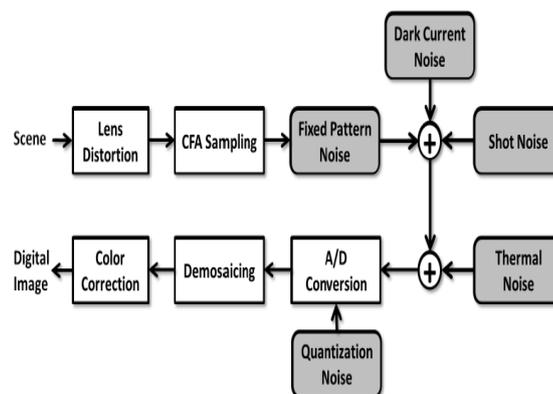
IMAGE DE-NOISE

The challenge of any image de-noising algorithm is to suppress noise while producing sharp images without loss of finer details. The first modern adaptive method to successfully address these contradictory goals can be attributed where the authors proposed a generalization of the SUSAN filter, which itself was an extension of the Yaroslavky filter. The authors there proposed de-noising by weighted averaging pixels similar in intensity within a local neighborhood. Under strong noise, identifying such similar pixels can be challenging.

memory locations in hardware or transmission in a noisy channel [1].

Removing impulse noise from images is a challenging image processing problem, because edges which can also be modeled as abrupt intensity jumps in a scan line are highly salient features for visual attention. Therefore, besides impulse noise removal, another important requirement for image de-noising procedures is that they should preserve important image structures, such as edges and major texture features.

Apart from the obvious reduction in image quality, such noise usually also hinders the performance of subsequent computer vision applications, such as tracking, object detection, etc. Suppressing such noise is, thus, the usual first step. However, before this can be performed, it is imperative to understand the source and characteristics of the corrupting noise. To do so, we

The problem of recovering patterns and structures in images from corrupted observations is encouraged in many engineering and science applications, ranging from computer vision, consumer electronics to medical imaging. In many practical image processing problems, observed images often contain noise that should be removed beforehand for improving the visual pleasure and the reliability of subsequent image analysis tasks. Images may be contaminated by various types of noise. Among them, the impulse noise is one of the most frequently happened noises, which may be introduced into images during acquisition and transmission. For example, it may be caused by malfunctioning pixels in camera sensors, faulty

briefly study the image formation pipeline (Fig. 1).

IMAGE FORMATION MODEL ILLUSTRATING THE VARIOUS NOISE SOURCES

While many algorithms have been developed to solve the problem of image enhancement, their performance has typically been evaluated only by comparing one method with another often in an ad-hoc manner. Over the years, many researchers have provided insight into the physics of either the fog or turbulence but not both. Most recently, researchers have proposed methods

to remove fog in images fast enough for real-time processing. Additionally, methods have been proposed by other researchers that address the atmospheric turbulence problem. We provide a new turbulent mitigation object metric that measures temporal consistency.

NOISE REMOVAL IN TURBULENCE

The noise removal in turbulence approach select a median filter simply because it can preserve edges reasonably well and it is data dependent thus adapts to the image signal. In order to reduce the complexity of our algorithm such that the processing speed is near real-time, we use a two dimensional median filter for each color channel for fast single image de-noising. It is important that the de-noising step is not too aggressive in reducing spatial frequencies because important details can be lost and unable to be recovered during the frame averaging and de-blurring steps. If noise removal is too aggressive, it effectively imposes premature bandwidth limitation and high frequency regions will be lost before the bandwidth recovery process (de-blurring). In this article, we use a very small window 3×3 for the median filtering step for de-noising.

Although median filter achieved the best performance in spike and Gaussian de-noising respectively, they are unsuitable for contemporary removal of different types of noise, because their best setting is noise-dependent. Vice versa, Median-modified Wiener filter (MMWF) that arrived second in each single de-noising category, was evaluated as the best filter for global de-noising, being its best setting invariant of the type of noise. In addition, median filter eroded the edge of isolated spots and filled the space between close-set spots, whereas MMWF because of a novel filter effect (drop-off-effect) does not suffer from erosion problem, preserves the morphology of close-set spots, and avoids spot and spike noise, an aberration encountered for Wiener filter.

IMAGE ALIGNMENT

The image alignment process proceeds in four steps. First, we perform a global translational alignment of each image to a single reference image using a full-frame alignment. Both the camera x, y translation and yaw and pitch rotation are modeled by translation, due to the orthographic projection model. The remaining z translation is irrelevant also due to the orthographic projection. Any camera roll is handled in the next step. Next, we average these globally aligned frames to produce a reference frame for the local alignment process. For each pixel in each image, we compute the sum-of-squared-differences (SSD) between the 3×3 neighborhood around the pixel and a corresponding translated window on the averaged image. The per pixel flow is chosen as the minimum SSD over 1/2 pixel discrete sampling within [-3; 3] pixels translation in x and y. This flow vector captures both the camera roll and atmospheric warping. Lastly, the global and local translations are added to determine the offset, for each pixel. These offsets are used to wrap each input image, using bilinear interpolation to produce a warped result. It should be noted that all computations are done in floating point to avoid further quantization errors.

IMAGE DEFOGGING

To remove fog effectively and efficiently for each frame and have an estimate of transmission, we use the Locally Adaptive Wiener Defogging method by Gibson and Nguyen [15]. In their work, the Wiener Defogging method is 50 to 100 times faster than existing methods and can operate at real-time speeds for frames of sizes 720 $\times$ 480 and larger.

A modification to the Wiener Defog method in order to automate the defogging process. The important step in removing fog with the Wiener Defogging method is the proper choice of size for the smoothing window size in the spatial domain. The optimal window size must be heuristically chosen for each image. This can be a cumbersome task for real-time video enhancements. The choice of window size is a common problem in single image defogging. A choice of two window sizes is needed to properly refine the transmission estimate but yet preserve depth discontinuities.

The dark channel prior is based on the following observation on haze-free outdoor images: in most of the non-sky patches, at least one color channel has very low intensity at some pixels. In other words, the minimum intensity in such a patch

should have a very low value. Formally, for an image *I*, we define

$$I^{dark}(x) \underset{c \in \{r,g,b\}}{min} \left(\underset{y \in \Omega(x)}{min} \left(I^c(y) \right) \right) \quad (4)$$

Where I_c is a color channel of *I* and $\Omega(x)$ is a local patch centered at *x*. Our observation says that except for the water color region, the intensity of *I* dark is low and tends to be zero, if *I* is a haze-free underwater image.

The low intensities in the dark channel are mainly due to three factors: a) shadows. e.g., the shadows of cars, buildings and the inside of windows in cityscape images, or the shadows of leaves, trees and rocks in landscape images; b) colorful objects or surfaces. e.g., any object (for example, green grass/tree/plant, red or yellow flower/leaf, and blue water surface) lacking color in any color channel will result in low values in the dark channel; c) dark objects or surfaces. e.g., dark tree trunk and stone

IMAGE DEBLUR

When the image *i(x)* has been defogged, motion compensated, and then frame averaged, the final step is to remove the blur caused by the atmosphere and image alignment errors (de-blur). In order to remove the blur, a kernel must be known. One approach is to apply a blind de-convolution method for isoplanatic conditions, the blur kernel is not exactly known but the structure is noted that there are two different forms of the optical transfer function (OTF), or blur kernel, due to turbulence: one for long exposure and the second for short exposure. The exposure time is in relation to the atmospheric turbulence. Short exposure measurements effectively "freeze" the turbulence during the image capture integration time. Only one instance of turbulence is captured in a short exposure frame.

CONCLUSION

Resolution loss and contrast loss are two of main types of degradation in Natural images. There are due to the effects of small angle forward-scattered light and back-scattered light respectively. Although both of these problems degrade the image quality, difficult is to mitigate than that of resolution loss. A new CETM method that is designed according our analysis on image alignment in low contrast and defogging with frame averaging. New turbulence mitigation metric (TMM) is developed that provides an objective measure for temporal consistency which is desired in turbulence mitigation. In this analysis, it is found that increasing contrast before tracking does not improve the performance when spatial noise is present. For removing turbulence it is common to average motion compensated images together in order remove the turbulent artifacts. Also it is discovered that removing fog before frame averaging is a better approach than removing fog after frame averaging because of the depth discontinuities in scenes. If there are no depth discontinuities then both approaches are the same.

REFERENCES

[1]. Anantrasirichai.N, Achim.A, Kingsbury.N, and Bull.D,(2013) "Atmospheric turbulence mitigation using complex wavelet-based fusion," IEEE Trans. Image Process., vol. 22, no. 6, pp. 2398–2408.

[2]. Bolme.D.S, Beveridge.J.R, Draper.B.A, and Lui.Y.M, (2010) "Visual object tracking using adaptive correlation filters," in Proc. IEEE Conf. CVPR, pp. 2544–2550.

[3]. Chan.S, Khoshabeh.R, Gibson.K, Gill.P, and Nguyen.T, (2011) "An augmented Lagrangian method for total variation video restoration," IEEE Trans. Image Process., vol. 20, no. 11, pp. 3097–311.

[4]. Carrano.C.J, (2003) "Anisoplanatic performance of horizontal-path speckle imaging," Proc. SPIE, vol. 5162, pp. 14–27.

[5]. Droege.D.R, Hardie.R.C, Allen.B.S, Dapore.A.J, and Blevins.J.C, (2012) "A real-time atmospheric turbulence mitigation and super resolution solution for infrared imaging systems," Proc. SPIE, vol. 8355, p. 83550R.

[6]. Farneback.G, (2000) "Fast and accurate motion estimation using orientation tensors and parametric motion models," in Proc. 15th ICPR, vol. 1, pp. 135–139.

[7]. Fried.D.L, (1966) "Optical resolution through a randomly inhomogeneous medium for very long and very short

84

M.Pavithra Devi, T.Maragatham, Karthik.S. et al., Inter. J. Int. Adv. & Res. In Engg. Comp., Vol.–03 (02) 2015 [80-84]

exposures," J. Opt. Soc. Amer. A, vol. 56, no. 10, pp. 1372–1379.

[8]. Gibson.K.S, Vo.D.T, and Nguyen.T.Q, (2012) "An investigation of dehazing effects on image and video coding," IEEE Trans. Image Process., vol. 21, no. 2, pp. 662–673.

[9]. Gibson.K and Nguyen.T, (2013) "Fast single image fog removal using the adaptive wiener filter," in Proc. 20th IEEE ICIP, pp. 714–718.

[10]. He.K, Sun.J, and Tang.X, (2009) "Single image haze removal using dark channel prior," in Proc. IEEE CVPR, pp. 1956–1963.

[11]. Joshi.N and M. F. Cohen, (2010) "Seeing Mt. Rainier: Lucky imaging for multi-image denoising, sharpening, and haze removal," in Proc. IEEE ICCP, pp. 1–8.

[12]. Koschmieder.H, (1940) "Luftlicht und sichtweite," Naturwissenschaften, vol. 26, no. 32, pp. 521–528.